

REPORT DOCUMENTATION PAGE

Form Approved
OMB No. 0704-0188

Public reporting burden for this collection of information is estimated to average 1 hour per response, including the time for reviewing instructions, searching existing data sources, gathering and maintaining the data needed, and completing and reviewing the collection of information. Send comments regarding this burden estimate or any other aspect of this collection of information, including suggestions for reducing this burden, to Washington Headquarters Services, Directorate for Information Operations and Reports, 1215 Jefferson Davis Highway, Suite 1204, Arlington, VA 22202-4302, and to the Office of Management and Budget, Paperwork Reduction Project (0704-0188), Washington, DC 20503.

1. AGENCY USE ONLY (Leave blank)	2. REPORT DATE	3. REPORT TYPE AND DATES COVERED
4. TITLE AND SUBTITLE		5. FUNDING NUMBERS

Nonlinear Optics in Novel Composite Media

61102F
2301/CS

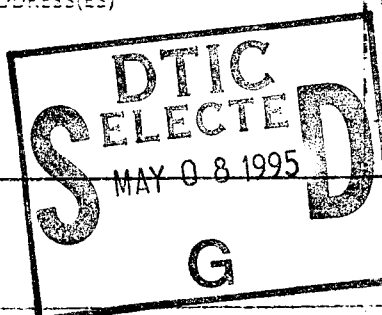
6. AUTHOR(S)	Professor Lawandy
7. PERFORMING ORGANIZATION NAME(S) AND ADDRESS(ES)	8. PERFORMING ORGANIZATION REPORT NUMBER

Dept of Engineering and Physics
Brown Univ
Providence, RI 02912

AFOSR-JR-95-0331

9. SPONSORING/MONITORING AGENCY NAME(S) AND ADDRESS(ES)	10. SPONSORING/MONITORING AGENCY REPORT NUMBER
AFOSR/NE 110 Duncan Avenue Suite B115 Bolling AFB DC 20332-0001	AFOSR-91-0107

11. SUPPLEMENTARY NOTES



12. DISTRIBUTION AND AVAILABILITY

APPROVED FOR PUBLIC RELEASE: DISTRIBUTION UNLIMITED

13. ABSTRACT (Maximum 200 words)

SEE FINAL REPORT ABSTRACT

19950505 172

DTIC QUALITY INSPECTED 5

14. SUBJECT TERMS	15. NUMBER OF PAGES		
17. SECURITY CLASSIFICATION OF REPORT	18. SECURITY CLASSIFICATION OF THIS PAGE	19. SECURITY CLASSIFICATION OF ABSTRACT	20. LIMITATION OF ABSTRACT
UNCLASSIFIED	UNCLASSIFIED	UNCLASSIFIED	UNCLASSIFIED

**Directorate of Physics and Electronics
Department of the Air Force
Air Force Office of Scientific Research (AFMC)
Bolling Air Force Base
Washington, DC 20332-6448**

**Final Report
AFOSR Grant No. AFOSR91-0107
December 1990 - June 1993**

“Nonlinear Optics in Novel Composite Media”

by

Principal Investigator:
Nabil M. Lawandy
Professor of Engineering and Physics
Brown University
Providence, RI 02912

Accesion For	
NTIS	CRA&I
DTIC	TAB
Unannounced	
Justification _____	
By _____	
Distribution / _____	
Availability Codes	
Dist	Avail and / or Special
A-1	

June 6, 1994

Summary of Accomplishments for the Grant Period 12/90 - 6/93

During this period of funding the research group has been more productive than ever. The research areas covered a variety of nonlinear optical phenomena in composite materials as well as several new spin-off areas. The group produced 40 papers in refereed journals and 28 conference presentations. In addition, three Ph.D. students will be graduated by the end of the grant period. Along with the Ph.D. students, there has been a vigorous undergraduate research involvement in the lab. The three undergraduates have all produced published research work which has or will appear shortly in journals. The rest of this section lists the group accomplishments under AFOSR funding, as well as the other vital statistics relating to the laboratory individuals and their accomplishments.

Publications--1990 - 1993

1. Lawandy, N. M., "What We Can Learn about Second Harmonic Generation in Germanosilicate Glass from the Analogous Effect in Semiconductor Doped Glasses," *Proceedings of the SPIE International Workshop on Photo-induced Self-Organization Effects in Optical Fiber*, p. 99-112, Vol. 1516, 1990.
2. Adler, C. L., and Lawandy, N. M., "Spectral and Temperature Dependence of the Nonlinear Index of Ruby Via Nondegenerate Two-Wave Mixing," *Optics Comm.* **81** (1,2), 33 (1991).
3. Adler, C. L., and Lawandy,N. M., "Viscosity of Picoliter Volumes Measured by Non-Degenerate Two-Wave Mixing," *Optics Comm.* **81** (1,2), 75 (1991).
4. Selker, M. D., and Lawandy, N. M., "Grating Formation in Frequency Doubling Fibers," *Journal de Physique* **1**, 1563 (1991).
5. Martorell, J., and Lawandy, N. M., "Spontaneous Emission in a Disordered Dielectric Medium," *Physical Review Letters* **66** (7), 887 (1991).
6. Lawandy, N. M., and MacDonald, R. L., "Optically Encoded Phase Matched Second Harmonic Generation in Semiconductor Microcrystallite Doped Glasses," *JOSA B* **8** (6), 1307 (1991).

7. Lawandy, N. M., Bernardin, J. P., Demouchy, G., and MacDonald, R. L., "Synchronous Pumping of a Picosecond Dye Laser Using Efficient Second Harmonic Generation in Germanosilicate Optical Fibers," *Electronics Letters* **27** (14), 1264 (1991).
8. Bernardin, J. P., and Lawandy, N. M., "Simultaneous Additive Pulse Mode Locking and Second Harmonic Generation of an Nd:YAG Laser Using Optically Encoded Germanosilicate Fibers," *IEE Proceedings--Journal of Optoelectronics* **138** (4), 281 (1991).
9. Adler, C. L., and Lawandy, N. M., "Measurement of the Diffusion Coefficient of Strongly Interacting Colloidal Suspensions by Nondegenerate Two-Wave Mixing," *Physical Review A* **43** (8), 4302 (1991).
10. Lawandy, N. M., Driscoll, T. J., and Adler, C. L., "A Test of Directional Photoionization Models of Second Harmonic Generation in Optical Fibers," *IEE(J) Journal of Optoelectronics* **139** (2), 133 (1991).
11. Afzal, R. S., and Lawandy, N. M., "Transverse Beam Reshaping and Beam Encoding by Two-Beam Coupling in Ruby," *Optics Comm.* **86** (3,4), 307 (1991).
12. Driscoll, T. J., and Lawandy, N. M., "Characterization of Second Harmonic Generation in Eu²⁺ Doped Aluminosilicate Optical Fibers," *Electronics Letters* **27** (19), 1729 (1991).
13. MacDonald, R. L., Driscoll, T. J., and Lawandy, N. M., "Second Harmonic Generation in Ion-Exchanged Semiconductor Doped Glass Waveguides," *Electronics Letters* **27** (1), 1717 (1991).
14. MacDonald, R. L., and Lawandy, N. M., "Tensor Properties of Optically Encoded Second Harmonic Generation in Semiconductor Doped Glasses," *Electronics Letters* **27**, 2331 (1991).
15. Driscoll, T. J., and Lawandy, N. M., "Observation of Frequency Doubling in Tantalum Doped Silica Fibers," *Electronics Letters* **27** (22), 2088 (1991).
16. Lawandy, N. M., "Comment on Polar Asymmetry of Photoionization by a Field with $\langle E^3 \rangle \neq 0$. Theory and Experiment," *Optics Comm.* **85**, 369 (1991).
17. Adler, C. L., and Lawandy, N. M., "Retarded Dispersion Forces in Periodic Dielectric Media," *Phys. Rev. Lett.* **66** (20), 2617 (1991).
18. Driscoll, T. J., Calo, J. M., and Lawandy, N. M., "Explaining the Optical Fuse," *Optics Letters* **16** (13), 1046 (1991).

19. MacDonald, R. L., and Lawandy, N. M., "Magnetic Field Effects in Optically Encoded Second Harmonic Generation in Germanosilicate Glasses," *J. Noncrystalline Solids* **141**, 47 (1992).
20. MacDonald, R. L., and Lawandy, N. M., "Optical Debye Effect," *Optics Comm.* **88**, 13 (1992).
21. Bernardin, J. P., and Lawandy, N. M., "Stable Modelocking of a Coupled Cavity Moving Mirror Ring Dye Laser," *Journal of Modern Optics* **39**, 457 (1992).
22. Driscoll, T. J., and Lawandy, N. M., "UV Enhancement and Erasure of Second Harmonic Generation in Germanosilicate Fibers," *Optics Letters* **17** (8) 572 (1992).
23. Cohen, J., and Lawandy, N. M., "Inductive High-Pass Filters for the Visible," *Applied Optics* **31** (16), 2974 (1992).
24. Lawandy, N. M., "Spontaneous Emission," McGraw-Hill Encyclopedia of Science, 1992.
25. Adler, C. L., and Lawandy, N. M., "Optical Gradient Forces on Colloidal Crystals: Generation of Spatially Complex Structures," *Optics Comm.* **91**, 354 (1992).
26. Lawandy, N. M., and Kweon, G., "Molecular and Free Electron Spontaneous Emission in Periodic Dielectric Structures," in C. M. Soukoulis, ed., Localization and Propagation of Classical Waves in Random and Periodic Structures, Plenum Press, New York, NY, 1992.
27. Bernardin, J. P., and Lawandy, N. M., "Experiments on Kinematic Modelocking of a Ring Dye Laser," *Optics Comm.* **94**, 445 (1992).
28. MacDonald, R. L., and Lawandy, N. M., "Observation of Charge Screening in Semiconductor Nanocrystals," *Physical Review B* **47** (4), 47 (1993).
29. MacDonald, R. L., Lawandy, N. M. and Khurgin, J., "Saturation of Near Resonant $\chi(3)$ ($0; 2\omega, -\omega, -\omega$) in Quantum Confined Semiconductors," accepted by *Physical Review B*.
30. MacDonald, R. L., and Lawandy, N. M., "Efficient Frequency Doubling at UV Wavelength in Optically Encoded Silicate Glasses," accepted by *Optics Letters*, 1992.
31. MacDonald, R. L., and Lawandy, N. M., "High Density Optical Storage Using Optically Encoded Second Harmonic Generation in Glasses," submitted to *Optics Letters*, November 1992.
32. Driscoll, T. J., and Lawandy, N. M., "Optically Encoded Second Harmonic Generation in Silicate Glasses," submitted to *JOSA B*, October 1992.

33. Kweon, G., and Lawandy, N. M., "Dispersion Interactions Between Excited Atoms," accepted by *Physical Review A*, 1992.
34. Bernardin, J. P., Gomes, A. S. L., Cohen, J. L., and Lawandy, N. M., "Experiments and Numerical Simulations on Beam Bending and Transverse Beam Encoding by Spatial Self and Cross-Phase Modulation in Ruby," submitted to *Optics Communications*, 1993.
35. Gomes, A. S. L., and Lawandy, N. M., "Stimulated Raman Scattering Externally Seeded by Molecular Spontaneous Emission," submitted to *Optics Letters*, 1993.
36. Kweon, G., Gomes, A. S. L., and Lawandy, N. M., "Superradiant Effects on the Absorption and Vibrational Heating of Polyatomics," submitted to *Journal of Chemical Physics*, 1993.
37. Driscoll, T. J., MacDonald, R. L., and Lawandy, N. M., "Helicity Effects in Second Harmonic Generation," submitted to *Physical Review A*, 1993.
38. Gomes, A. S. L., Balachandran, R. M., and Lawandy, N. M., "Nonlinear Absorption in Photodarkened CdS_xSe_{1-x} Doped Glasses," submitted to *Optics Communications*, 1993.
39. Driscoll, T. J., and Lawandy, N. M., "Sum Frequency Generation in Silicate Glass," submitted to *Optics Letters*, 1993.
40. Lawandy, N. M., "Comment on 'Fluorescence-Lifetime Measurements in Monodispersed Suspensions of Polystyrene Particles,'" submitted to *JOSA B*, 1993.

Conference Presentations--1990 - 1993

1. Lawandy, N. M., and Adler, C. L., "Picoliter Viscosity Measurements Using Nondegenerate Two-wave Mixing," Paper No. MTT6, OSA Annual Meeting, Boston, MA, November 4-9, 1990.
2. Lawandy, N. M., and Adler, C. L., "Chaotic Crystals," Paper No. TuP1, OSA Annual Meeting, Boston, MA, November 4-9, 1990.
3. Lawandy, N. M., and MacDonald, R. L., "The Optical Debye Effect," Paper No. WV6, OSA Annual Meeting, Boston, MA, November 4-9, 1990.
4. Lawandy, N. M., and Adler, C. L., "Measurement of the Diffusion Coefficient of Strongly Interacting Colloidal Suspensions by Nondegenerate Two-Wave Mixing," Paper No. QMC4, QELS, Baltimore, MD, May 13-19, 1991.

5. Lawandy, N. M., Driscoll, T. J., and MacDonald, R. L., "Second Harmonic Generation in Semiconductor Doped Glass Waveguides," Paper No. JTdB3, QELS, Baltimore, MD, May 13-19, 1991.
6. Lawandy, N. M., and MacDonald, R. L., "Optically Encoded Second Harmonic Generation in Semiconductor Microcrystallite-Doped Glasses," Paper No. JTdB5, QELS, Baltimore, MD, May 13-19, 1991.
7. Lawandy, N. M., Adler, C. L., Bernardin, J. P., Driscoll, T. J., and MacDonald, R. L., "A Test of Directional Photo-Ionization Models for SHG in Optical Fibers," Post Deadline Paper, QELS, Baltimore, MD, May 13-19, 1991.
8. Adler, C. L., and Lawandy, N. M., "Retarded Dispersion Interactions in Periodic Structures," Paper QOWe26, European Quantum Electronics Conference, Heriot-Watt University, Edinburgh, Scotland, August 27-30, 1991.
9. MacDonald, R. L., and Lawandy, N. M., " $\chi^{(2)}$ Tensor Properties and Multiwavelength Erasure Rates for Optically Encoded Second Harmonic Generation in Semiconductor Microcrystallite Doped Glasses," Paper No. MSS3, OSA Annual Meeting, San Jose, CA, November 3-8, 1991.
10. Driscoll, T. J., and Lawandy, N. M., "Characterization of Frequency Doubling in Eu²⁺ Doped Silica Fibers," Paper No. MSS1, OSA Annual Meeting, San Jose, CA, November 3-8, 1991.
11. Driscoll, T. J., and Lawandy, N. M., "SHG Patterns from Optically Encoded Bulk Glasses: Evidence for Optical-Phase and Polarization Dependent Charge Drift," QELS, Anaheim, CA, Paper JTdB4, p. 46.
12. Driscoll, T. J., and Lawandy, N. M., "Non-Exponential and Non-Ohmic Thermal Erasure of $\chi^{(2)}$ Gratings in Borosilicate Glass," OSA, Albuquerque, NM, 1992, Paper TuB3.
13. Driscoll, T. J., and Lawandy, N. M., "Fundamental and Second Harmonic Dependence of the Optical Encoding of $\chi^{(2)}$ Gratings in Borosilicate Glass," OSA, Albuquerque, NM, 1992, Paper TuB5.
14. MacDonald, R. L., and Lawandy, N. M., "Observation of Charge Screening in Semiconductor Nanocrystals," OSA, Albuquerque, NM, 1992, Paper TuP4.
15. Bernardin, J. P., and Lawandy, N. M., "Experiments in Kinematic Modelocking," OSA, Albuquerque, NM, 1992, Paper WU5.
16. Kweon, G., and Lawandy, N. M., "Molecular Interactions and Line Broadening in Electromagnetically Confined Geometries," QELS, Anaheim, CA., 1992, Paper QWG7.

17. Kweon, G., Beadie, G., and Lawandy, N. M., "Pyroelectric Detection of Light Beams Using a Phase Transition in Guest-Host Compounds," OSA, Albuquerque, NM, 1992, Paper MHH7.
18. Selker, M. D., Lawandy, N. M., and Driscoll, T. J., "Low-pump Power Fiber Seeded Raman Capillary System," OSA, Albuquerque, NM, 1992, Paper ThN4.
19. MacDonald, R. L., and Lawandy, N. M., "Efficient Frequency Doubling into the UV in Silicate Glasses," OSA, Albuquerque, NM, 1992, Paper PD22.
20. Kweon, G., and Lawandy, N. M., "Cerenkov Emission in Photonic Bandgap Structures," OSA, Albuquerque, NM, 1992, Paper PD26.
21. Driscoll, T. J., and Lawandy, N. M., "Optical Encoding of a Same Frequency Grating in Silica Based Glass," OSA, Toronto, Canada, 1993, Paper C-00314.
22. Driscoll, T. J., MacDonald, R. L., and Lawandy, N. M., "Helicity Dependence of Optically Encoded Second Harmonic Generation," OSA, Toronto, Canada, 1993, Paper C-00313.
23. Beadie, G., Sauvain, E., Gomes, A. S. L., and Lawandy, N. M., "Temperature Dependence of Carrier Dynamics in $\text{CdS}_x\text{Se}_{1-x}$ Doped Glasses Studied by Two Color Picosecond Spectroscopy," OSA, Toronto, Canada, 1993, Paper A-00062.
24. Beadie, G., and Lawandy, N. M., "Molecular Spontaneous Emission in a Dielectric Hard Sphere Gas," CLEO, Baltimore, MD, 1992, Paper QTuC3.
25. Gomes, A. S. L., Cohen, J. L., Bernardin, J. P., and Lawandy, N. M., "Anisotropic Nonlinear Propagation in Ruby: Beam Fission and Optically Induced Bending," CLEO, Baltimore, MD, 1992, Paper CThD7.
26. MacDonald, R. L., and Lawandy, N. M., "Saturation of Near Resonant $\chi^{(3)}(0; 2\omega, -\omega, -\omega)$," CLEO, Baltimore, MD, 1992, Paper QThH36.
27. MacDonald, R. L., and Lawandy, N. M., "High Density Optically Encoded Information Storage Using Second Harmonic Generation in Glass," CLEO, Baltimore, MD, 1992, Paper CFA3.
28. Driscoll, T. J., and Lawandy, N. M., "Pre-Excitation and Temporal Correlation Studies on the Optical Encoding of $\chi^{(2)}$ Gratings in Silica Based Glasses," CLEO, Baltimore, MD, 1992, Paper QFA5.

Invited Talks/Honors

Electro-Optics Seminar Series, Goddard Space Flight Center, March 1990:
 "Second Harmonic Generation in Germanosilicate Glasses"

Physics Colloquium at the Polytechnical University, Brooklyn, NY, September 1990:
"Spontaneous Emission in Random and Periodic Dielectric"

Electrical Engineering Seminar at The Johns Hopkins University, October 1990:
"Radiative Processes in Periodic Dielectrics"

Seminar at Bellcore, Red Bank, NJ, January 9, 1990:
"Molecular QED in Periodic and Random Dielectrics"

Physics Colloquium, Brown University, February 25, 1990:
"Molecular Radiative Processes in Dielectric Structures"

Invited Talk at the International Conference on Photo-Induced Self-Organization Effects in
Optical Fibers, Laval University, Quebec City, Canada, May 10, 1991.
"What Can We Learn about SHG in Homogeneous Glasses from the Analogous Effect in
Semiconductor Doped Glasses?"

Invited Talk at the Progress in Electromagnetics Research Symposium, M.I.T., July 1, 1991.
"Photonic Bandgap Effects in Colloidal Crystals"

Condensed Matter Seminar at University of Toronto:, October 28, 1991:
"Spontaneous Emission, Laser Action and Vacuum Compression in Colloidal Crystals"

Invited to participate in a Panel Discussion on the Status of Second Harmonic Generation in
Glasses at OSA Annual Meeting, San Jose, CA, November 5, 1991.

Physics Colloquium at Worcester Polytechnic Institute, December 9, 1991:
"Spontaneous Emission in Random and Periodic Colloids"

Invited to participate as a Panelist at the ARO/NASA Workshop on Photonic Bandgaps in
Utah, January 1992

Invited lecture at the Gordon Conference on the Physics of Polyelectrolyte Solutions,
February 1992:
"Consequences of Photonic Bandgaps in Colloidal Crystals"

Invited lecture at the APS Annual Meeting in Indianapolis, IN, March 1992:
"Spontaneous Emission and Laser Action in Colloidal Systems," Paper G53

Physics Colloquium at Brandeis University, March 1992:
"Second Harmonic Generation in Glasses: Physics and Applications"

Invited lecture at the NATO Conference on Photonic Band Structure and Localization, Crete,
Greece, May 1992

Invited Speaker at the New England Meeting of the AAPT, U. S. Coast Guard Academy,
November 1992:
"Spontaneous Emission in Ordered and Random Colloids"

Physics Colloquium at Rensselaer Polytechnic Institute, December 8, 1992:
"Second Harmonic Generation in Bulk Glasses"

Appointed to the Editorial Board of *Optics Communications*, January 1992.

Science News article covering the work on "Inhibited Spontaneous Emission in Periodic Structures," *Science News* 138, 196 (1990).

Science News article about the work on the "Fiber Fuse," *Science News* 140, 200 (1991).

Science magazine article discussing our experimental work on the inhibition of spontaneous emission in colloidal crystals, *Science* 255 (5051), 1512 (20 March 1992).

Discover magazine article discussing our work on vacuum fluctuations in periodic structures, *Discover*, March 1992, p. 112.

Scientific American article discussing our work on photonic bandgaps and their potential for photocatalysis, *Scientific American*, May 1992, p. 28.

Ph.D. Students and Undergraduate Research

The AFOSR grant funding which began 12/90 was instrumental in supporting the Ph.D. research of five graduate students. Three of the students, Robert L. MacDonald., Timothy J. Driscoll, and James P. Bernardin, will complete their dissertations and graduate this year. Robert MacDonald has defended his thesis and will begin research at NEC Research Laboratories on microcavity lasers this summer. Timothy Driscoll has been offered postdoctoral positions by Professor Christos Flytzanis in France and by Dr. C. Gilbreath at NRL. James Bernardin will be finishing late this summer and is likely to receive an offer from Dr. James Abshire of NASA GSFC. The titles of the Ph.D. theses are listed below:

Robert L. MacDonald

"Optically Encoded Second Harmonic Generation in Semiconductor Microcrystallite Doped Glass: Physics and Applications"

Timothy J. Driscoll

"Fundamental Studies of the Second Harmonic Generation in Bulk Silicate Glasses"

James P. Bernardin

"Kinematic Modelocking of Dye Lasers and Two Beam Coupling in Birefringent Nonlinear Media"

Undergraduate research was an important part of the laboratory function and the use of AFOSR funds. As always, there are several undergraduates participating in their own projects complementing the research work. Over the grant period, the primary students were Jason Cohen, Joe Greenberg, and Jayson Cohen. Jason Cohen did work on developing an inductive high pass filter for submicron wavelengths. His work resulted in a paper in Applied Optics. Jayson is now working at a software company in the Bay area. Joe Greenberg did his senior thesis in the lab on laser-driven flocculation of colloids. He also investigated solvent induced chirality in C₆₀. Joe graduated and is now a fellowship student in the Cornell Applied Physics program. The third student, Jayson Cohen, worked on nonlinear beam propagation in ruby, coherent backscattering from disordered media, C₆₀ oxidation reactions, and developed optical limiter using C₆₀ in polymers. Jason published two papers and will be attending the University of Michigan next year.

Current Laboratory Personnel

Sabbatic Visitor

Professor Anderson S. L. Gomes
Universidade Federal de Pernambuco, Brazil

Post-Doctoral Fellows

Dr. Evelyne Sauvain
Institute of Microtechnology, Neufchatel, Switzerland

Ph.D. Students

J. P. Bernardin	4th year (Engineering)
T. J. Driscoll	4th year (Physics)
G. Kweon	4th year (Physics)
R. L. MacDonald	4th year (Physics)
G. Beadie	3rd year (Physics)
R. M. Balachandran	3rd year (Physics)

Undergraduates

J. L. Cohen

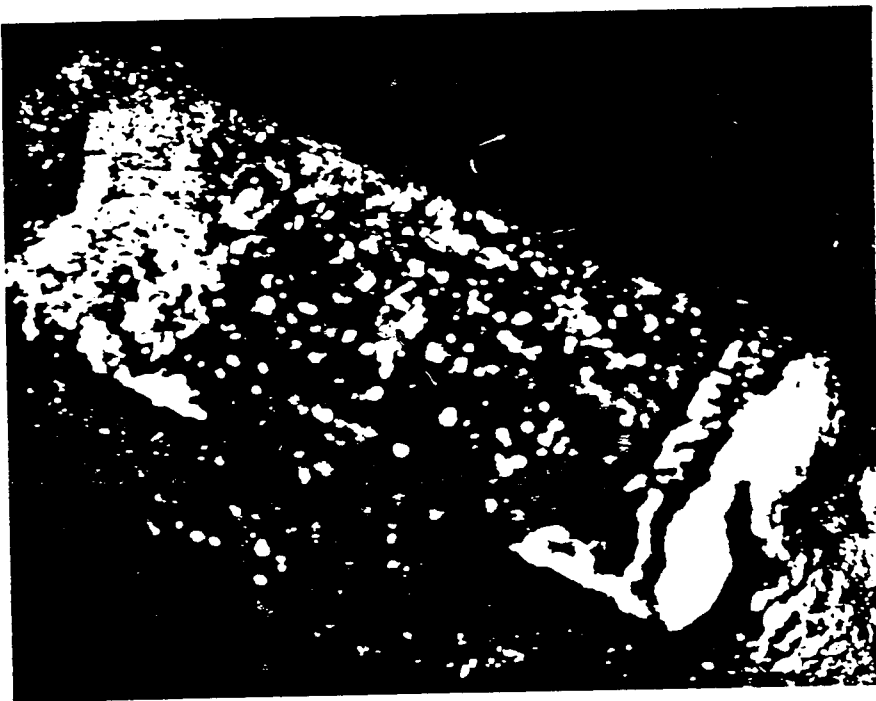
J. Cohen

J. Greenberg

I. Applied Research

Pyroelectric Detection Using Molecular Guest-Host Complexes

During the past year we have succeeded in experimentally realizing one of the several potential applications of molecular guest-host structures such as the β -quinol: χ clathrate system, where χ represents some guest complex for the β -quinol host matrix. The measurements were made using small single crystals of the β -quinol:CH₃OH clathrate contacted to electrodes normal to the c-axis. The mounted crystal is shown in the photo below.



1 mm
→ ←
Mounted Sample

Using these crystals in an He dewar, we were able to observe modulated pyroelectric response at a variety of laser wavelengths from the visible to the far IR. We expected this behavior to occur below the phase transition temperature since

there exists a macroscopic polarization in this phase. This pyroelectric signal was indeed observed and was found to be strongest at 55K. During the course of the measurements, a completely unexpected pyroelectric signal was observed above the transition temperature. This signal, shown in Figure 1, was found to peak at 80K and continued up to 150K. Although the strong pyroelectric signal at temperatures above liquid nitrogen is not yet explained, it has drastic implications for the use of these materials. These materials can now be directly employed as sensitive pyroelectric detectors at temperatures available to thermoelectric and liquid nitrogen reservoir coolers.

A comparison was made of the potential pyroelectric performance of these materials and conventional pyroelectrics. The quantity most often used to do this is the pyroelectric figure of merit, R_v . A comparison of the figure of merit for different materials revealed that the β -quinol:CH₃OH system is comparable to TGS+analine and LiTaO₃, two of the best materials known to date. Based on this comparison and the many possible combinations of host complexes and guest molecules, we believe that inclusion compound systems should be able to improve greatly upon conventional pyroelectric detectors.

Temperature Dependence of the Pyroelectric Response

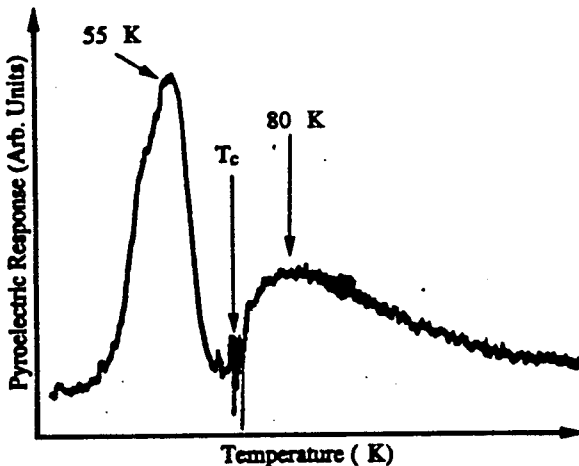


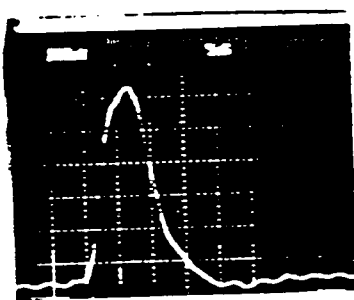
Figure 1

- Above T_c there shouldn't be a pyroelectric response because the CH₃OH dipoles are expected to be randomly oriented.

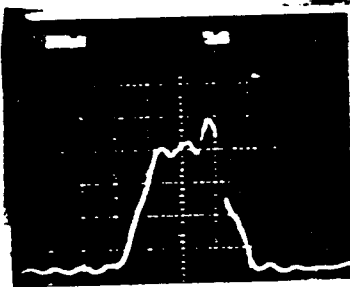
Optical Limiter Action and Oxidation Chemistry of C₆₀ in Organic Polymers

Optical activity induced by Buckminster fullerenes can be exploited when these molecules are introduced into polymers or porous glasses (i.e., Vycor or SolGel glasses). The C₆₀ guest molecule provides a large magneto-optical response as well as rapid inter system crossing and excited state absorption to induce optical limiter action. Important considerations include chemical stability of the C₆₀ molecule in host environment and impregnation of the guest structures.

Fast limiter action is required in the laser warfare environment for hardening of optical devices and personnel protection. C₆₀ and C₇₀ have large excited state absorption originating from the rapidly populated triplet state. We have demonstrated optical limiter action in transparent polymers using 5 nanosecond pulses at 532 nm (Energy Fluence = 1 J/cm²). Figure (2) demonstrates the limiter action of the bucky-polymer.



Input Laser Shape



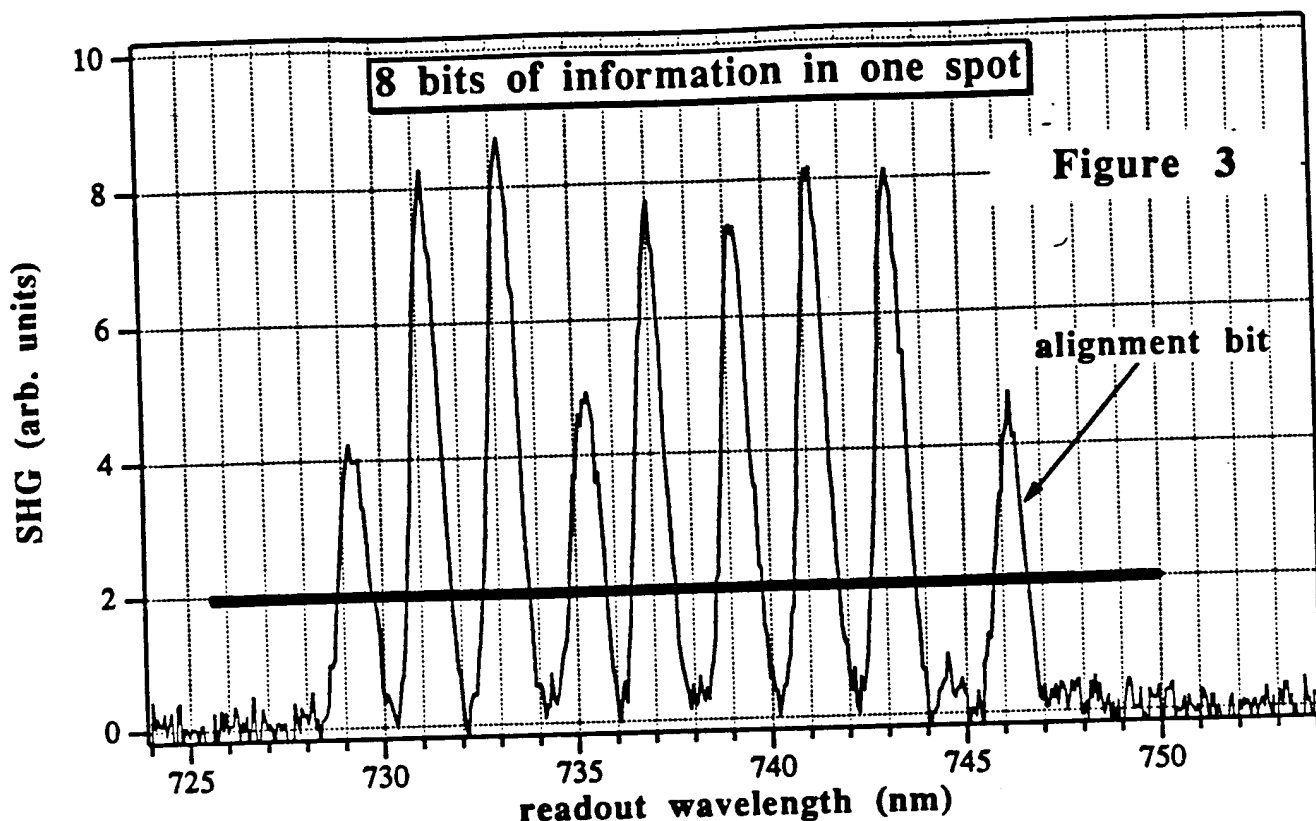
Pulse Shape after propagation through 1 cm of Bucky Polymer

Figure 2

Fullerene degradation due to oxygen reactions with the host restricts the possibilities for nonlinear optical applications. We are the first to observe rapid destruction of both C₆₀ and C₇₀ fullerenes in a large number of organic solvents, including polymer forming materials. This work directly impacts the preparative stages needed to produce composite media from organic polymer hosts and the fullerene series.

High Density Optical Information Storage in Glasses

Based on our discovery of optically encoded second harmonic generation in bulk homogeneous and semiconductor doped glasses, we experimentally demonstrated that these systems could be used at fundamental wavelengths as short as 600 nm, thus producing UV second harmonics. In the course of the experiments, which utilized tunable dye lasers for encoding, we discovered that more than one quasi-phase matched grating could be encoded in a single spot of the glass. This discovery led us to the question of how many separately readable gratings could one write? The answer was the astounding result that a separate grating could be written every 4 Å of the fundamental wavelengths in commercial silicate glasses. Using the dye laser output and its second harmonic, we experimentally demonstrated that 28 gratings could be written in a single 14 μm × 14 μm spot of SK5 glass with only 15 nm of bandwidth. An example of the readout wavelength dependence for a spot with 9 bits of information encoded in it is shown in Figure 3. In addition to encoding the glass, we have demonstrated that erasure of the $\chi^{(2)}$ gratings could be affected by either UV light exposure or thermal cycling. This write-erase cycle can be repeated multiple times with no significant degradation of the material.



The ability to store and readout information in the frequency domain in a rugged and low-cost material such as glass opens up a very exciting possibility for a new high-density optical storage medium. Based on our findings, we believe that these glasses can be used to encode information in the form of second harmonic $\chi^{(2)}$ gratings with densities in excess of one Gigabyte/cm². In addition, our theoretical modeling of the process shows that dispersion at the second harmonic dramatically increases the possible $\chi^{(2)}$ grating density per unit frequency. Based on this fact, along with their ability to be rapidly encoded, semiconductor microcrystallite composite glasses will be the focus of on-going research. In this system the sharp semiconductor band edge produces much sharper dispersion at 2ω than transparent glasses. Calculations for this system predict that we will be able to encode information using single shots of laser energy with a density in excess of 10^{10} bits/cm².

Second-Harmonic Generation in Semiconductor Doped Glass Waveguides

We have observed efficient second-harmonic generation (SHG) in ion-exchanged semiconductor doped glass (SDG) waveguides. Interest in nonlinearities of these waveguides arises from their potential application to all-optical integrated signal processing devices. Since the first report of these SDG waveguides in 1986, work has focused on third order nonlinearities, with applications to optical switching and bistability. We extend this work to second-harmonic generation using the recently discovered seeded preparation in SDG, and we study self-preparation in these waveguides.

These semiconductor doped glasses possess no second order nonlinearity due to the macroscopic inversion symmetry of the material. However, an effective $\chi^{(2)}$ can be encoded by simultaneous exposure to the fundamental and second-harmonic beams. This effective $\chi^{(2)}$ most likely results from a dc field which changes sign at the phase matching length. The encoding process is believed to be due to carriers promoted into the conduction band of the microcrystallites and swept to long-lived surface traps by a resonance enhanced $\chi^{(3)}(0;\omega,\omega-2\omega)$ generated dc field within the crystallite. When the encoding fields are removed, a net dc field is left across the microcrystallite creating an effective $\chi^{(2)}_{\text{eff}} = \chi^{(3)}E_{\text{dc}}$. The quasi-phase matching extends throughout the length of the samples and has provided conversion efficiencies of 10^{-6} in bulk SDG.

Waveguides were fabricated using a 400°C solution of KNO_3 and Na containing glasses. This ion-exchange resulted in channels 5cm long and $2\mu\text{m}$ deep. They were prepared for SHG in the same manner as bulk SDG with the fundamental and second-harmonic fields coupled into the guiding structure using prisms. We used a frequency doubled Q-switched modelocked (76 MHz) Nd:YAG laser, which produced 120 ps and 80 ps pulses at $1.06\ \mu\text{m}$ and 532 nm, respectively. The frequency conversion was observed by coupling into the waveguide only 1.06

μm radiation and filtering the output beam with an IR high reflector and a 532 nm band pass filter. Experiments were also conducted to study the effects of self-preparation, using the SHG contribution from the waveguide side wall interface as the seed signal.

This work demonstrates the possibility for large-scale integrated optic devices using bichromatic logic in similar systems where ion-exchanged gratings may provide the coupling into or out of the device anywhere on the glass surface. In addition, high efficiency SHG should be possible in these waveguides by providing long concentric, ring waveguide structures on a single planar piece of SDG.

Improved Conversion Efficiencies and New Frequency Doubling Fibers

Although bulk glass provides the best situation for an experimental investigation of the frequency doubling phenomenon, optical fibers have the advantage of providing high intensities and long interaction lengths. In an attempt to improve conversion efficiencies, we have explored pre-treatment of fibers and searched for new fiber systems which could be encoded for efficient SHG. We have shown that UV irradiation at 355 nm lowers the preparation threshold in SK5 and enables germanosilicate fibers to be encoded with cw laser light. One germanosilicate fiber in our laboratory which has a dopant level of 10^{-3} Nd³⁺ has exhibited conversion efficiencies of 7% after UV pre-treatment. In the quest for new fiber systems, we have studied europium doped aluminosilicate fibers. The aluminum oxide (Al₂O₃) is necessary to raise the refractive index of the core while the rare earth dopant Eu^{2+/3+} allows for frequency doubling with a stability of <±5%. Tantalum doped silica is another system we have discovered which may be optically encoded. In this system the tantalum oxide dopant is responsible for both the guiding properties of the fiber and the frequency doubling capability. More

recently, we have also shown that praseodymium doped aluminosilicate fibers also exhibit efficient SHG.

Discovery of Thermally Driven Spontaneous Damage in Germanosilicate Fibers and the Optical Fuse

Germanium oxide doped fibers carrying power densities of the order of 1.0 MW/cm² display a catastrophic damage phenomenon when contacted at the fiber tip. The damage propagates at speeds of the order of 1.0 cm/sec back to the input end of the fiber and leaves behind a quasi-periodic pattern of elongated bubbles. Due to the bright flash associated with the phenomenon and the destruction of the core for further light propagation, this effect has been named the optical fuse.

Initial theories assumed an interplay between the light and glass material to explain the fuse. Our experiments demonstrated, however, that the same damage pattern could be generated by simply heating the fiber to 700-1000°C. Since these temperatures are below the melting point of silica and calorimetry experiments determined that the propagating fuse is characterized by temperatures above 2,000°C, we claim that an exothermic chemical reaction is responsible for the damage. Several exothermic reactions are possible in the germanosilicate fiber between germanium defects and oxygen. Based on measurements of the diffusion of O₂ in glass, an activation energy of the order of 1.0 eV was determined supporting the explanation that the optical fuse is a thermally driven process as well. The discovery that catastrophic damage can result in an optical fiber at temperatures as low as 700°C has important ramifications for the use of these materials in sensor applications. Of particular importance is their use in feedback control information in high risk environments such as nuclear power plants. Our work on this problem was the subject of a feature article in *Science News* (Vol. 140).

Simultaneous Self-Starting Additive Pulse Mode-Locking and Second Harmonic Generation of an Nd:YAG Laser Using Self-Organized Germanosilicate Optical Fibers

Several reports of self-starting additive pulse modelocking (APM) of solid state lasers have appeared recently. These include diode pumped Nd:YAG and Ti:Al₂O₃ lasers. The nonlinear cavities used in these experiments were formed using single mode optical fibers as the nonlinear medium. The fibers are typically of the order of one meter long or less, and along with the reflector, provide the intensity dependent reflectivity required to trigger and sustain modelocked operation. The use of fibers for the nonlinear index medium for APM presents a second exciting possibility of simultaneously frequency doubling and tripling the laser output. This combined process is made possible by the well known but not well understood phenomena of second harmonic generation in germanosilicate optical fibers. Fibers which have been self-prepared or conditioned using seeded preparation have resulted in conversion efficiencies as high as 13% when used outside a laser cavity. Experiments on a c.w. Nd:YAG laser which is passively modelocked using a conditioned germanosilicate fiber external cavity for APM and SHG are discussed. The external cavity reflector is 100% reflecting at 1.06 μm and 90% transmitting at 532 nm. The coupled cavity laser emits pulses at 532 nm which are shorter than 5 psec.

Nonlinear Propagation in Anisotropic Crystals: Beam Fission and Optically Induced Bending in Ruby

Spatial ring pattern formation due to transverse self-phase modulation has been observed in several materials including ruby, GdAlO₃:Cr³⁺, and photorefractive materials. Induced transverse effects due to beam coupling have also been demonstrated in ruby, whereby rings present on a strong pump beam

were transferred to a weak probe beam of different wavelength. Most of the reported studies have been performed with the incident beams polarized parallel or perpendicular to the crystal's c-axis, thus avoiding anisotropic effects. We performed theoretical and experimental studies of nonlinear beam propagation in ruby, where novel transverse effects were observed due to self- and induced-action in the anisotropic regime. These effects are shown to arise from the large n_2 associated with the charge transfer band dispersion in the \bar{E} state of ruby.

A cw argon laser tuned to 515 nm with a maximum power of 1.5W was focused to a 140 μm diameter spot. The beam was normally incident on a 7 cm long ruby rod (Cr^{3+} density of $1.1 \times 10^{19} \text{ cm}^{-3}$). For the two-beam experiments, an He-Ne (< 1mW) was used as the probe beam, co-propagating with the pump. The two beams were simultaneously polarized before the lens. The transmitted beams (pump and probe) were spatially analyzed in the far field as a function of incident polarization, pump power and rod position relative to the focus. At a fixed power and polarization with respect to the c-axis, different spatial profiles were observed for the rod face positioned before (converging input beam), after (diverging input), and at the lens focus. When the beams are carefully aligned and focused on the rod face, with polarizations parallel to c ($I_p//c$), ring formation is readily observed in both pump and probe beams. If, however, the pump beam is spatially shifted with respect to the probe beam, induced bending of the probe is observed regardless of the focus position relative to the rod face. In addition, rings are encoded in both beams for incidence at and after the focus. A bending angle of 5.5 mrad was measured at 1.95 kW/cm² pump intensity.

Another interesting effect occurs when the input polarization is rotated. When the incident polarization is rotated by 60° from the $I_p//c$ position, the pump beam develops a side spot, which evolves from the ring pattern as the power is increased. As the input polarization is rotated from $I_p//c$ to $I_p\perp c$, the side spots are

very clear at 45°, 60°, and 75°, and an input intensity-dependent energy exchange process, which has been studied in detail, takes place between the two spots.

While the self-and-induced effects at I_p/c (or $I_p \perp c$) can be modeled by a full computation of the nonlinear wave equations, including self- and cross-phase modulation terms, the behavior in the anisotropic regime requires a complete vector simulation to account for our experimental observations, which has also been performed.

High Efficiency Stimulated Raman Scattering In Gases Using External Seeding Processes

The conversion efficiency of stimulated Raman scattering (SRS) is limited by the fact that the process builds up from spontaneous emission noise. The system used to overcome this limiting effect utilizes nonlinear frequency conversion in a glass fiber to produce a seed for the SRS, and it uses a capillary tube to confine the pump light in the gas. The experimental set-up includes a cell containing CH₄ at 560 lb/in², pumped at 532 nm by using a mode-locked, Q-switched, and frequency doubled Nd:YAG laser. With an average power of approximately 50 mW of the pump light split off to the fiber to produce the seed, a change in the intensity of the first Stokes line at ~630 nm was clearly visible. This corresponded to a conversion efficiency of 22% with only 40 mW of pump power at a Q-switch rate of 450 Hz. At higher powers a sizable anti-Stokes emission at 460 nm was also generated. The large conversion efficiency of this unoptimized system demonstrates the feasibility of SRS for obtaining multiple wavelengths with diode pumped laser systems.

An extension of the above technique to a regime of longer pulse width and higher energy uses the broad spontaneous emission generated by a dye cell as the seeding beam.

The pump radiation was provided by the second harmonic of a Nd:YAG laser (532 nm, 7 ns, 5Hz). Part of the beam was diverted to pump a dye cell operated without any feedback mirrors, whereas the remaining energy was focused by a $f = 80$ cm lens to a stainless steel 1.25 m long cell filled with CH_4 (vibrational shift 2914 cm^{-1}) at 30 atm. The pump energy was varied up to 50 mJ using polarizers while the seeding beam was provided by emission from a cell containing Rhodamine 640 in methanol (10^{-3}M) pumped by 2 mJ. From the total output energy of the broadband (6.09 THz centered at 629 nm) dye emission, only $18 \mu\text{J}$ was injected into the Raman cell to seed the emission. The Raman bandwidth of CH_4 at 30 atm being 19.3 GHz, only $0.06 \mu\text{J}$ of the seed energy was being used. An estimate of the total available energy in the solid angle from spontaneous Raman scattering at our experimental parameters near threshold (7 mJ pump energy) gives an approximate value of 20 pJ, to be compared to the value of 60 nJ provided by the useful fluorescence in the seeding beam.

There is a factor of over twenty for both output energy and efficiency near the threshold for 1st Stokes generation from seeded to unseeded and the power required for 1st Stokes generation with 1% efficiency was reduced due to seeding by a factor of almost 2. However, at the power where 1% efficiency (unseeded) was achieved (~15 mJ), an almost 10-fold increase was measured for seeded Raman. Similar behavior occurred for the output energy. Also noticeable was the increase in efficiency for 2nd Stokes and 1st anti-Stokes generation due to the seeding of the 1st Stokes.

Kinematic Modelocking of a Ring Dye Laser

New experimental results on a coupled cavity moving mirror ring dye laser operating with a repetition rate of 250 MHz were obtained. Figure 4(a) shows the picosecond pulse train and Figure 4(b) shows the millisecond envelope.

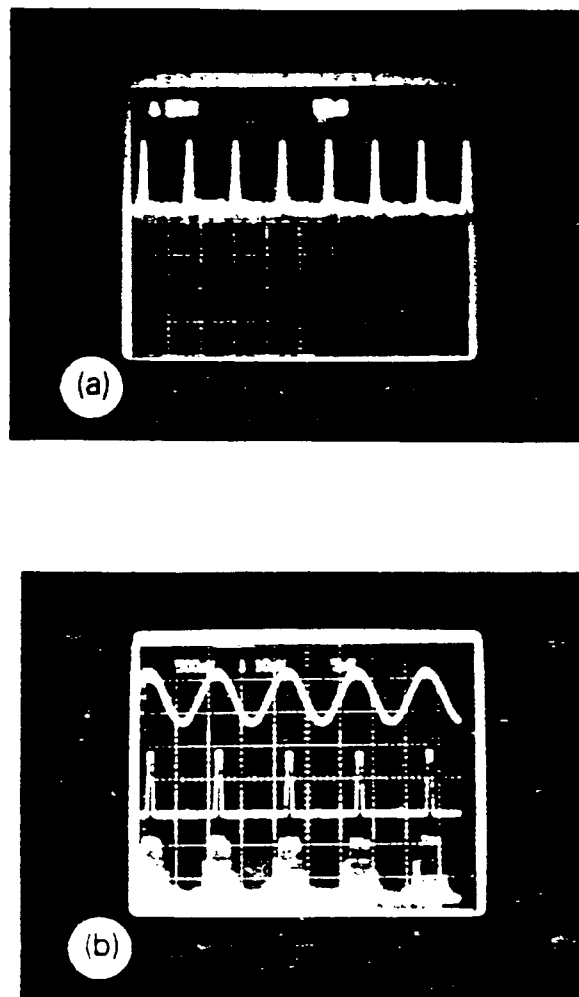


Figure 4

Existing models for the modelocking mechanism are analyzed in light of the results of various experiments performed in this study. We found that thresholds exist for the onset and instability of kinematic modelocking (KML) as a function of pump power. The pulse length dependence on mirror velocity and cavity detuning was determined, and asymmetries in the mirror velocity were found. In addition, we found that the width of the cavity beatnote at 250 MHz is not in fact correlated with the required mirror velocities for modelocking as some models have conjectured. It is shown that the Doppler shift required to achieve KML is

approximately equal to the peak frequency pulling induced by the gain medium. A prism pair is added to the external cavity for group velocity dispersion compensation which with proper adjustments can also tune the laser over the entire Rhodamine 6G bandwidth. With the inclusion of prisms in the external cavity, the modelocking is found to be more stable with pulses shorter than 3 psec being produced by the KML mechanism.

Development of a Picoliter Viscometer

Nondegenerate two-wave mixing (NDTWM) has been previously used to measure the relaxation time of solid-state systems. In an artificial Kerr medium, the relaxation time is the time for a particle to diffuse a portion of the index grating induced by radiation-pressure forces. This time is proportional to the viscosity of the medium. Our work demonstrates the use of NDTWM as a viscometer for picoliter volumes. Experiments were performed to measure the viscosity of suspensions of 0.090 μm diameter polystyrene microspheres titrated with known quantities of water and glycerol. Good quantitative agreement with tabulated values was found for the viscosity of water-glycerol solutions. Unlike viscometer techniques, which typically require large volumes of fluid, this technique can be implemented with fewer than 50 pL of sample volume, making it ideal for biological and medical applications.

II. Basic Research

Theory of Nonlinear Optical Properties of Crystalline Guest Host Complexes

A class of inclusion compound known as clathrates are ideal systems for studying the alteration of spectral characteristics of small atoms and molecules due to quantum confinement. Such characteristics include the observation of previously forbidden transitions and the observation of recoil effects when the translational states of the center of mass are not eigenstates of the momentum operator.

Theoretical studies of the rattling motion of rare gas atoms in a clathrate such as β -hydroquinone have been performed by modeling the host-guest potential with a Poschl-Teller potential, for which an exact solution to the Schrodinger equation can be found. It is shown that a dipole moment induced in the guest, due to the variation of the potential over the extent of the guest, is responsible for the IR activity of the rattling motion, with the effective dipole moment approximately proportional to the potential strength and the mean square radius of the guest. Low temperature far IR spectra of β -quinol clathrates with nitrogen guests have yielded absorption coefficients, due to this rattling motion, which show fair agreement with predictions. Also, due to the anharmonicity of the potential, the zero to three overtone transitions, although weak, will not be strictly forbidden. This indicates the presence of a third-order susceptibility for third harmonic generation, which is calculated and compared with that of other media, which have been shown to exhibit third harmonic generation in the far IR.

For molecular guest species the asymmetric variation of the potential will also alter the change in the dipole moment with interatomic spacing, thereby altering the spectral characteristics of vibrational motion. Vibrational lines of normally gas phase active molecules, such as CO, have been observed to shift when

enclathrated. We have examined the induced change in the dipole moment of gas-phase inactive molecules, such as N₂ and O₂, to examine the possibility of observing induced IR activity when these species are enclathrated.

For strong internal transitions whose wavelength is comparable to the cage size 4-5 Å, recoil becomes an important effect. In the harmonic limit the impulsive change in momentum should produce a spatially coherent state. However, anharmonicity and short lifetimes of the higher lying states will limit the coherence of the final state. The possibilities of observing signatures of spatial coherence, such as characteristic translational energy shifts of the emitted x-ray and far-IR emission from the decay back to the ground state, are examined.

Second Harmonic and Sum Frequency Generation in Silica Based Glass

Many glass materials simultaneously irradiated with fundamental laser light and its second harmonic may be optically encoded for efficient second harmonic generation (SHG). This self-organizing effect has been observed in a variety of glasses over a range of wavelengths. The encoding process is believed to break symmetry by creating a permanent spatially periodic internal electric field (E^{dc}). The dc field acts on $\chi^{(3)}(-2\omega; \omega, \omega, 0)$ to quasi-phase-match the frequency doubling process. The physics explaining the formation of the $\chi^{(2)}$ grating has eluded researchers since the first observation in optical fibers in 1981. In an attempt to extract the microscopics of this puzzling phenomenon we have focused on: (1) work involving new bulk glass materials for efficient second harmonic generation, (2) UV irradiation effects on the encoding process, and (3) determination of the transverse symmetry of E^{dc} by analyzing the radiated second harmonic free space mode and $\chi^{(2)}$ tensor symmetries. We have also just succeeded in encoding a sum frequency grating in silica based glass.

Initial studies on SHG in glass led researchers to believe that this was a phenomenon restricted to germanosilicate fibers. Our work in 1989 on germanosilicate fiber preforms, however, demonstrated that this was a fundamental property of bulk germanosilicate glass. This discovery ruled out any models based on the waveguiding properties of fibers and freed experimentalists from fiber complications such as group velocity dispersion, self- and cross-phase modulation, and weakly guiding modes. Shortly thereafter we also demonstrated that this is a general phenomena of silica based glass and not just germanosilicate fiber preforms. We have shown that lead oxide and barium oxide doped silica glasses may also be encoded for efficient SHG. By working with bulk glasses with a thickness less than the Rayleigh length of our encoding beams, we were able to accurately study the intensity dependence of the writing process. This work has demonstrated a threshold in the preparation intensities of the order of 1.0 GW/cm^2 for barium oxide doped silica glass (SK5) and 1.0 MW/cm^2 for the lead oxide doped glass (F8). This threshold behavior is an important part of any suggested theory and casts serious doubt on any models relying upon interference between excitation channels of a low number of photons.

Pre-irradiating the SK5 glass with average 355 nm intensities of 3 W/cm^2 lowers the preparation threshold to $\sim 1.0 \text{ MW/cm}^2$. The uv light was provided by a frequency tripled Q-switched Nd:YAG laser operating at $1.064 \mu\text{m}$, which emitted 30 mJ uv pulses at a rate of 20 Hz ($P_{\text{peak}} = 7.5 \text{ MW}$). The 1.0 mm samples, which were exposed for ten minutes to the uv radiation prior to preparation, displayed a preparation threshold at much lower intensities and an overall enhanced conversion efficiency. Carvalho et al. discovered that germanosilicate fibers simultaneously exposed to 266 nm radiation during the encoding process improved the conversion efficiency. They also showed that the effect of the 266 nm light was not permanent and that delaying the preparation pulses by 1 ms caused a much lower enhancement. The improvement in SK5 is permanent and more reminiscent of a similar effect on the IR preparation

threshold we have observed in germanosilicate fibers pre-irradiated with 200 W/cm² of cw 351.1 nm light. Untreated germanosilicate fibers demonstrate a preparation threshold similar to SK5, after uv irradiation, however, a permanent change to the fiber allows for $\chi^{(2)}$ gratings to be written with cw laser light.

Preparation of the bulk glass showed that the second harmonic was radiated in either a solid or a higher order free-space mode depending upon the writing beam intensities and their relative polarization. This is extremely important since solid Gaussian modes were used to encode and read-out the $\chi^{(2)}$ gratings. Using symmetry arguments and a knowledge of the writing and reading mode symmetries, we can deduce the spatial distribution of the possible internal electric fields which would allow coupling to the various free-space modes. The solid lowest order modes used to encode and read-out the $\chi^{(2)}$ gratings serve to constrain the symmetry of the product of the transverse mode radiated and the transverse structure of the encoded $\chi^{(2)}$. At low intensities above the rapid turn on points alluded to earlier, it was discovered that depending on which tensor component was analyzed the radiated second harmonic mode was observed in a different higher order mode. By combining the observed mode symmetry with an analysis of the encoded $\chi^{(2)}$ tensor components, we can obtain a clearer picture of the internal electric fields responsible for the frequency doubling. Figure 5 displays the various modes radiated for each tensor component analyzed from gratings encoded with orthogonal or linear polarizations.

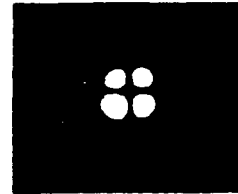
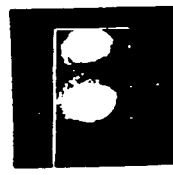
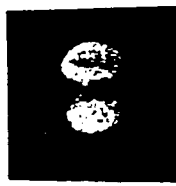
In order to extract the $\chi^{(2)}$ tensor symmetries, we begin with the x- and y-components of the radiated second harmonic which obey the relations

$$|E_x(2\omega)|^2 \approx |\chi_{xxx} \cos^2 \theta + 2\chi_{xxy} \cos \theta \sin \theta + \chi_{xyy} \sin^2 \theta|^2 \quad (1)$$

Radiated Patterns in Silica Based Glass

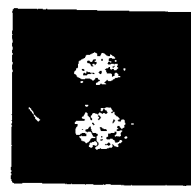
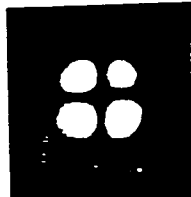
parallel polarizations

unanalyzed



χ_{xxx}

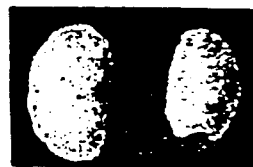
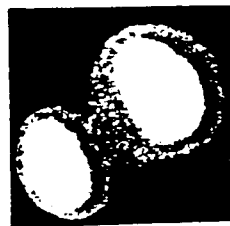
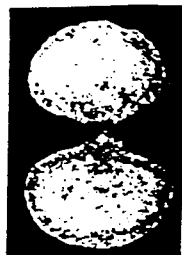
χ_{yxx}



χ_{xyy}

χ_{yyy}

orthogonal polarizations



χ_{xxx}

---->

χ_{yyy}

Figure 5

$$|E_y(2\omega)|^2 \approx |\chi_{yyy} \sin^2 \theta + 2\chi_{yyx} \cos \theta \sin \theta + \chi_{yxx} \cos^2 \theta|^2 \quad (2)$$

where Θ is the read-out beam polarization measured with respect to the vertical x-axis and the coefficients are effective $\chi^{(2)}$ tensor components dependent on the overlap integral:

$$\chi_{ijk_{eff}}^2 \approx \int_0^\infty \int_0^{2\pi} \chi_{ijk}^{(2)}(r, \phi) E^2(\omega) E^*(2\omega) r dr d\phi \quad (3)$$

The evaluation of this overlap integral requires a knowledge of the free-space mode of the second harmonic and the read-out beam and critically depends on the symmetry of the $\chi^{(2)}$ tensor. Since we are assuming that the grating is established by an electric field acting on $\chi^{(3)}(-2\omega; \omega, \omega, 0)$, we can replace $\chi^{(2)}$ in this integral with $\chi_{ijk}^{(2)} - \chi_{ijkl}^{(3)} E_1^{dc}$. Since the existing $\chi^{(3)}$ components are known for centrosymmetric materials, it is possible to determine the transverse field components of E_1^{dc} . This investigation has determined that E^{dc} is created by a charge flux that is predominantly radial in nature for encoding at lower intensities, but at higher intensities the charge flux is directed along the polarization direction of the second harmonic encoding beam creating a field with a constant direction across the read-out beam axis.

Recently we have demonstrated the ability to optically encode a sum frequency generation grating in SK5 by simultaneously irradiating the glass with ω , 2ω , and 3ω . When the grating was read out with ω and 2ω , a signal at 3ω was detected. We are currently investigating the encoding characteristics of this new phenomenon.

Carrier Screening Effects in Semiconductor Microcrystallite-doped Glass Second Harmonic Generation

We studied the dependence of optical erasure rate on intensity for above bandgap erasure ($\hbar\omega > E_g$) of SHG in semiconductor microcrystallite-doped glasses encoded for SHG. The results were found to be consistent with directional trapping of free carriers, excited by the erasure beam, which cancel out the encoded d.c. field. The intensity dependence was measured on OG 530 (Schott Glass Co., $hc/E_g \sim 530$ nm) erased with 514.5 nm radiation from a cw argon ion laser. The measured erasure rates decrease with increasing intensity over the range 6 - 12 W/cm². The lower limit intensity corresponds to one pair of free carriers per crystallite and to a Debye screening length comparable to the crystallite diameter ($d \sim 200\text{\AA}$). This strong screening of the frozen-in field is due to high carrier densities produced by the erasure beam and results in a decreased erasure rate. Further increasing the erasure beam intensity increases the carrier density and results in a slower random erasure process above 20 W/cm².

Saturation of Near Resonant $\chi^{(3)}$ (0;2 ω ,- ω ,- ω) in Quantum Confined Semiconductors

Semiconductor microcrystallite-doped glasses (SDG), which do not have a macroscopic $\chi^{(2)}$ due to the random orientation of microcrystallites within the glass host, can be optically encoded to exhibit phase-matched second harmonic generation (SHG) in a manner similar to seeded preparation of homogeneous glass. The simultaneous exposure of the SDG to radiation at the fundamental and second harmonic is believed to leave behind a d.c. electric field with the proper spatial periodicity to phase-match a $\chi^{(3)}(-2\omega;\omega,\omega,0)$ process. The SDG are believed to be encoded in a three-step process involving directional trapping of free carriers

generated by absorption of the second harmonic and directed by $E_{dc} = \chi^{(3)}(0; 2\omega; -\omega, -\omega) E^2(\omega) E(2\omega)$. When the encoding fields are removed, a d.c. electric field is left behind, and the SHG is a direct measure of the strength of the d.c. field and an indirect measure of $\chi^{(3)}(0; 2\omega; -\omega, -\omega)$.

Steady-state encoding efficiencies were measured in several types of SDG encoded with known fundamental and second harmonic intensities ($I(\omega), I(2\omega)$) from a modelocked (120 ps at 1.06 μm), Q-switched and frequency doubled Nd:YAG laser. The results indicate that there exists an optimal $I(2\omega)$ which is relatively insensitive to E_g , the semiconductor bandgap energy, and to the value of $I(\omega)$ used during encoding. The steady-state encoding efficiency can be diminished by both a change in the phase-matching condition and a decrease in $\chi^{(3)}(0; 2\omega; -\omega, -\omega)$. Measurements on different length samples show that the optimum value of $I(2\omega)$ is independent of thickness, ruling out phase-matching effects.

The observed intensity dependence $I(2\omega)$ of the encoding efficiency indicates that $\chi^{(3)}(0; 2\omega; -\omega, -\omega)$ saturates with absorption at 2ω , providing strong evidence that $\chi^{(3)}(0; 2\omega; -\omega, -\omega)$ is dominated by doubly resonant terms, which are non-zero due to quantum confinement of the electron and hole states in the semiconductor nanocrystals. Calculations of such doubly resonant contributions to $\chi^{(3)}$ in the small homogeneous broadening limit lead to:

$$\chi^{(3)}(0; 2\omega, -\omega, -\omega) = \frac{1}{2\pi^3} \alpha(2\omega) \lambda_{2\omega} \frac{\hbar^2}{m_0 \Gamma} \frac{m_0}{\mu} \left(\frac{e}{\hbar \omega} \right)^2 \quad (1)$$

where $\alpha(2\omega)$ and $\lambda_{2\omega}$ are the microcrystallite absorption coefficient and the wavelength at the second harmonic frequency, respectively, Γ is the homogeneous broadening, and μ is the electron-hole reduced effective mass. When this $\chi^{(3)}$ is used in a rate equation model for the encoding process, which takes into account the

change in $\chi^{(3)}$ during an encoding pulse, the equilibrium encoded electric field becomes:

$$E_{dc}(I_{2\omega}) \propto \frac{x^{1/2}(1-e^{-x})^2}{x+e^{-x}-1} \quad (2)$$

where $x = \frac{I(2\omega)T_p}{E_{sat}}$, T_p is the encoding Q-switched pulse width, and E_{sat} is the saturation energy density at 2ω . Using values for E_{sat} from absorption saturation measurements in the model developed, we obtain a theoretical expression for the encoding efficiency versus $I(2\omega)$, which is in good agreement with the data.

Cerenkov Emission in a Photonic Bandgap Crystal

A simple model of the Cerenkov emission in a periodic structure with a 3-D photonic bandgap is considered. For the dispersionless case, a uniform dielectric slab would emit all the frequencies in a cone with the same angle. When a photonic bandgap is present, the emission wavelength becomes a strong function of the angle. In the case of a more realistic photonic bandgap calculation, the multivalley structure of the bands would result in a more complicated but symmetric chromatic emission pattern with different colors being emitted along characteristic directions. Calculations were performed for a 15% filling fraction crystal with a peak density-of-states corresponding to an index of refraction ratio 3.5. In this case, an enhancement of about a factor of ten in the density-of-states (DOS) is expected from numerical band structure calculations. It is found from the calculation that the peak radiated power scales at the bandedge density of states and that this can be comparable or exceed the power radiated by a uniform dielectric. This latter point presents a particularly interesting possibility for slowing down charged particle beams by purely radiative means. This could be accomplished using the photonic

structure described by Yablonovitch et al., which is formed by the intersection of channels which extend through the entire crystal. In the visible region, the channels would be of the order of 100 nm in diameter allowing for the unimpeded passage of a collimated electron beam. This concept may prove useful for the particle detectors, reactor moderators, and stimulated Cerenkov lasers.

Dispersion Interactions Between Excited Atoms

The complete quantum electrodynamic calculation of the dispersion interaction for the case of two ground state atoms was well-developed by the 1950's. A case which to our knowledge has not been studied is that of two excited multi-level atoms. A most general expression for the interaction energy between two identical atoms which is valid in the dipole approximation shows that new phenomena such as oscillation and repulsion can exist in multi-level atoms. The final expression for the interaction energy is far too lengthy to present here. Instead the well-known results for two ground state atoms was compared to those of two multi-level atoms which are both in the same excited state. Because of its popularity in laser cooling and trapping experiments, Na in its 3p state is compared to Na in its 3S state. The calculations were performed using a nine-level model of the sodium atom, with the seven levels above 3p accounting for most of the oscillator strength from bound transitions. When the separation is comparable to λ_{ge} , the transition wavelength between the ground state and the first excited state, the potential exhibits a substantial repulsive barrier. Similar calculations were performed for two Cs atoms in the 6p state and again a repulsive potential barrier was found at $R \approx \lambda$, where λ is the 6s - 6p transition wavelength (865.9 nm). These barriers correspond to temperatures of 7.3 mK for Na and 78 mK for Cs, which can be well above those accessible by laser cooling methods.

Superradiance Effects on the Vibrational Fluorescence of Optically Pumped Molecules

Experiments based on laser induced fluorescence (LIF) have shown that in certain molecules internal degrees of freedom such as vibration can equilibrate on time scales considerably shorter than those required for V-T and V-R equilibration. We have experimentally demonstrated that superradiant emission on a rotational line can strongly affect the vibrational temperature and fluorescence of these molecules when pumped by intense IR lasers. Experiments were performed on $^{14}\text{NH}_3$ pumped on its $a(6,0) \rightarrow s(7,0)$, $v_2, v = 0 \rightarrow 1$ transition by the 9R16 line of a self-modelocked CO₂ TEA laser. The CO₂ line center is 0.04 cm⁻¹ below the absorption line and leads to intense FIR emission at 90.6 μm, near resonant with the $s(7,0) \rightarrow a(6,0)$ transition in $v_2, v = 1$. This emission is a highly efficient Raman-like process. In order to measure the effects of the superradiant process on the equilibration of the NH₃ vibrational modes, the fluorescence from the $(n+1)v_1 \rightarrow nv_1$ band at 3.4 μm was monitored through the side of the cell using a filtered Golay cell. Using D₂O which absorbs at 90.6 μm and is transparent to the CO₂ pump, we were able to suppress the build-up of the superradiant NH₃ emission. Addition of the D₂O into the cell changed the CO₂ pump absorption and the fluorescence signal from high lying vibrational states. The conclusion is that the presence of the self-generated superradiant emission makes the CO₂ pumping process more efficient and results in a significantly higher vibrational temperature and excited state fluorescence.

Light Driven Complex Structures in Colloidal Media

Work on deterministic instabilities and chaos over the past decade has largely focused on spatio-temporal behavior. In connection with fluids and, more

recently, laser dynamics, spatial structures have played an increasingly important role. In this work we show that standing light waves, which can exert periodic radiation forces on dielectric particles, can be used to produce complex structures in colloidal crystals of polystyrene spheres. The crystals are formed by a strong repulsive Debye-potential interaction in ultraclean aqueous environments having particle densities on the order of $10^{14}/\text{cm}^3$. Quasi-elastic laser-light scattering measurements show that the crystals assume a face-centered cubic lattice with a (111) plane separation of several thousand angstroms. The injection of a standing optical wave produces a second periodic potential, which in one-dimensional results in the well-studied circle mapping for the position of the nth ball: $X_{n+1} = X_n + a + \sin 2kx_n$, where a is the unperturbed lattice spacing and is proportional to light intensity. We have studied the phenomenon in two-dimensional and three-dimensional systems and will show that the light forces available from cw lasers can produce "chaotic crystals," as well as other solutions, for certain winding numbers and intensities.